Available online at www.sciencedirect.com
SCIENCE DIRECT®
Bioorganic & Medicinal Chemistry Letters 14 (2004) 3715–3720
Bioorganic & Medicinal Chemistry Letters

# Structure-based design of amidinophenylurea-derivatives for factor VIIa inhibition

Otmar Klingler,* Hans Matter, Manfred Schudok, Monica Donghi, Joerg Czech, Martin Lorenz, Hans Peter Nestler, Hauke Szillat and Herman Schreuder

*Aventis Pharma Deutschland GmbH, Building G878, D-65926 Frankfurt, Germany*

Received 3 February 2004; accepted 6 May 2004

**Abstract**—The amidinophenylurea scaffold was earlier shown to provide an excellent template for the synthesis of novel and potent inhibitors of the blood coagulation factor VIIa. In this contribution we describe the structure-based design of potent ligands guided by X-ray crystallography, molecular modeling and docking studies. The design and synthetic efforts were directed towards novel modifications to explore the protease binding region close to the S4 subsite.


Blood coagulation not only plays a crucial role in haemostasis after tissue injury, but also in the pathogenesis of many thrombotic events. The tissue factor/factor VIIa (TF/fVIIa) complex is the physiological activator of the coagulation system and catalyzes the proteolytic activation of factors X and IX. The activated factor X, in turn, activates prothrombin to thrombin that converts fibrinogen to fibrin. Since the TF/fVIIa complex is the key initiator of this process, it is a promising target for future antithrombotic strategies.[1–3]

In a previous paper, we reported the identification of a novel series of amidinophenylureas as potent inhibitors of factor VIIa.[4] The X-ray structure of the factor VIIa/tissue factor complex with compound **1** at 2.2 Å resolution revealed several features, which seem important for high affinity to factor VIIa (Fig. 1). In addition to the amidinophenyl binding to Asp189 in S1, both urea NH's interact with the active triad Ser195-Oγ, either directly or via a structurally conserved water. This initial X-ray structure displayed a phenyl ring stacked on top of the imidazole ring from the active triad His57 directed towards the factor VIIa S2 pocket. The following optimization revealed that smaller, hydrophobic substituents fit better into this rather small pocket, while others also reported polar interactions to key residues within this pocket.[5] The subsequent optimization strategy was based on this X-ray structure and docking studies using FlexX and QXP.[6,7]

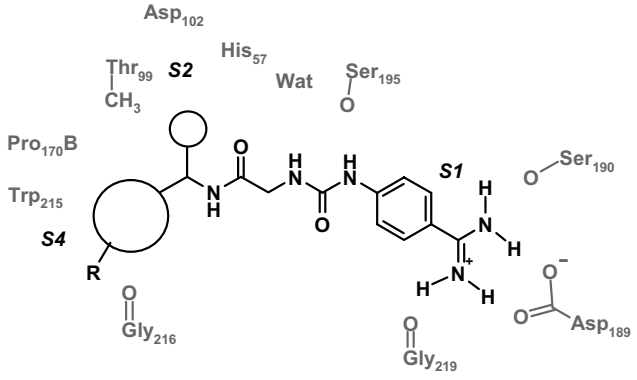


**Figure 1.** Schematic key protein–ligand interactions of compound **1** to the fVIIa binding site, as derived from X-ray structure of **1** in complex with human fVIIa and tissue factor (**1**, $K_i = 0.73\,\mu M$).

Our initial compounds did not place substituents towards the open factor VIIa S4 pocket to gain affinity and selectivity, as it is now suggested by X-ray crystallography and our binding hypothesis from docking studies. This binding hypothesis stimulated our search for more potent factor VIIa inhibitors in this series by investigating further structural features to explore this particular pocket.

*Keywords*: Factor VIIa; Thrombosis; Serine protease.
* Corresponding author. Tel.: +49-(0)69-305-83313; fax: +49-(0)69-305-21618; e-mail: otmar.klingler@aventis.com

0960-894X/$ - see front matter © 2004 Elsevier Ltd. All rights reserved.
doi:10.1016/j.bmcl.2004.05.006

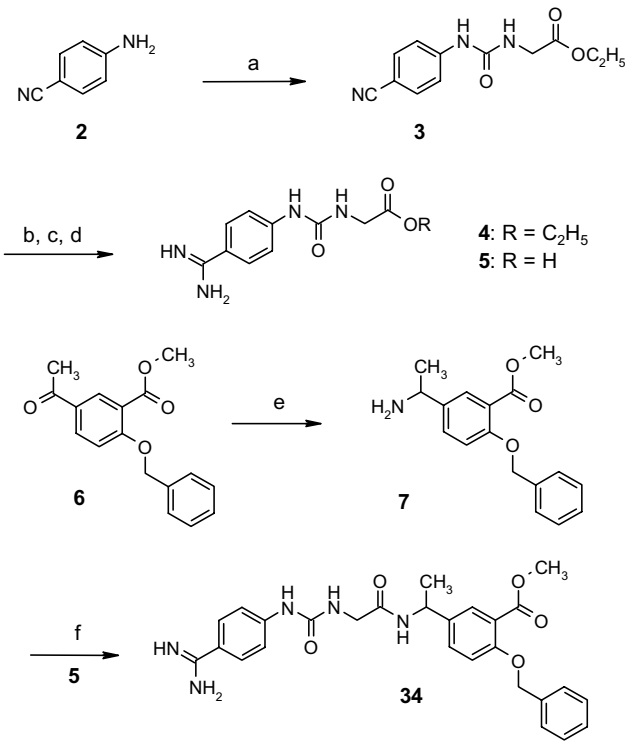


**Scheme 1.** Synthesis of compound **34**. Reagents: (a) ethoxycarbonylmethyl isocyanate, DMF; (b) HCl, EtOH; (c) $NH_3$, EtOH; (d) NaOH, $H_2O$; (e) MeOH, $NaCNBH_3$, $NH_4OAc$; (f) TOTU, DMF, N-ethylmorpholine.

The synthetic pathway used for the preparation of the compounds **1**–**36** is outlined in Scheme 1 representatively, for example, **34** and is in accordance to the methods described in our previous paper.[4]

Aminobenzonitrile **2** was reacted with ethoxycarbonylmethyl isocyanate to provide the corresponding urea **3**, which was subjected to a Pinner reaction to give amidinophenylurea **4** and subsequently converted to the acid **5**.[8] Coupling of the key intermediate **5** with amine **7** proceeded readily to give compound **34**.[9] Most of the amine building blocks were generated analogously to amine **7** by reductive amination of ketone precursor **6**.

Our initial studies unveiled the influence of the S2 directed substituent $R^1$, as summarized in Table 1. Binding affinities for the inhibitors **9**–**36** are expressed as inhibition constants $K_i$ towards fVIIa and structurally related serine proteases.[10]

The first compounds in Table 1 support our previous results.[4] Introduction of a methyl group in the benzylic position (α-position) of compound **9** resulted in the racemic compound **10** with a marked increase in potency (**10**, $K_i = 0.077\,\mu M$). For selected molecules, both enantiomers were separated and tested. In general, the *S*-enantiomer is more active. This, for example, is indicated by comparing compound **11** and **12**. The *S*-enantiomer **11** is found to be ~300-fold more potent than the *R*-enantiomer **12**, which is in agreement with modeling studies and subsequently confirmed by the X-ray structure. The small α-methyl substituent of compound **11** in its complex with factor VIIa/tissue factor thoroughly fits into the S2 pocket.

**Table 1.** In vitro activity for compounds **9**–**17**

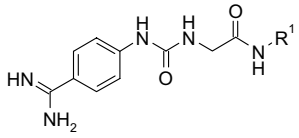


| Compounds | $R^1$ | $K_i$ (μM) | | |
|---|---|---|---|---|
| | | fVIIa | fXa | Thrombin |
| **9** | 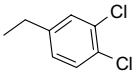 | 0.97 | 14.5 | 10.1 |
| **10** | 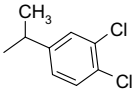 | 0.077 | ND | ND |
| **11** | 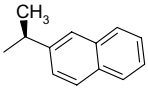 | 0.026 | 6.23 | 3.18 |
| **12** | 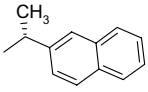 | 7 | ND | ND |
| **13** | 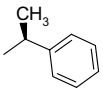 | 0.43 | >10 | 50.7 |
| **14** | 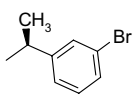 | 0.027 | >10 | 15.9 |

**Table 1** (*continued*)

| Compounds | $R^1$ | $K_i$ (μM) | | |
|---|---|---|---|---|
| | | fVIIa | fXa | Thrombin |
| **15** | 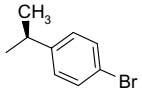 | 0.156 | >10 | 6.76 |
| **16** | 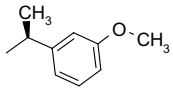 | 0.035 | >10 | 18.2 |
| **17** | 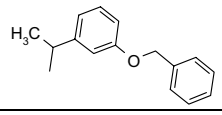 | 0.256 | ND | ND |

ND: not determined.

This encouraging result prompted us to design a novel series of S4 directed amidinophenyl ureas containing the essential methyl group in α-position. Since the S4 pocket was found to be relatively flat, solvent exposed and featureless, a diverse set of substituents at the α-methyl benzylamide core was selected to explore this region.

Compared to the α-*S*-methyl benzylamide **13** ($K_i = 0.43\,\mu M$), the replacement of phenyl by naphthyl yielded a marked increase in binding affinity of compound **11** ($K_i = 0.026\,\mu M$), which may be attributed to favourable hydrophobic interactions of the second aromatic ring in the factor VIIa binding site area 4.5 Å from Gly216. This is consistent with the finding that bromine at this position in **14** also increases affinity ($K_i = 0.027\,\mu M$) while bromine in *para*-position led to compound **15** with a $K_i$ of $0.156\,\mu M$. The subsequent exploration by additional *meta*- and *para*-substituted analogues revealed steric constraints imposed by the Ser214-Trp215-Gly216-Gln217 β-sheet in the factor VIIa binding site and confirms that small and hydrophobic substituents are well accepted in the *meta*-position. The *meta*-methoxy substituent in **16** still can undergo favourable hydrophobic interactions ($K_i = 0.035\,\mu M$), while the bulkiness of the larger *meta*-benzyloxy substituent in **17** decreases affinity to $0.256\,\mu M$.

A second hydrophobic or polar ring $R^2$ was introduced in *para*-position of the α-methyl benzylamide by direct link or linkers like carboxamides and ethers. The biological activities of these derivatives are given in Table 2.

The *para*-benzyloxy derivative **18** ($K_i = 0.133\,\mu M$) and *para*-phenyloxy derivative **19** ($K_i = 0.078\,\mu M$) demonstrate the favourable effect of larger hydrophobic substituents directed towards S4 in comparison to **13**. The replacement of the ether oxygen in **19** by $CH_2$ in **20**

**Table 2.** In vitro activity for compounds **18**–**33**

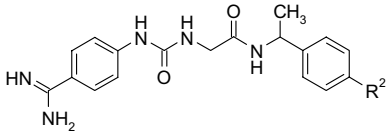

| Compounds | $R^2$ | $K_i$ (μM) | | |
|---|---|---|---|---|
| | | fVIIa | fXa | Thrombin |
| **18** | 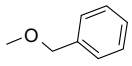 | 0.133 | ND | ND |
| **19** | 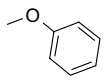 | 0.078 | >10 | 9.1 |
| **20** | 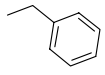 | 0.190 | ND | ND |
| **21** | 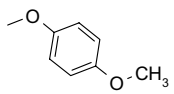 | 0.083 | 10.7 | 9.8 |
| **22** | 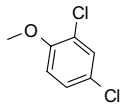 | 0.483 | ND | ND |

(*continued on next page*)

**Table 2** (*continued*)

| Compounds | $R^2$ | $K_i$ (μM) | | |
|---|---|---|---|---|
| | | fVIIa | fXa | Thrombin |
| **23** | 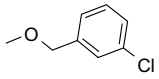 | 0.023 | >10 | 2.3 |
| **24** | 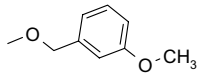 | 0.020 | >10 | 2.3 |
| **25** |  | 0.142 | >10 | 3.2 |
| **26** | 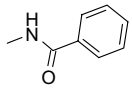 | 0.034 | 4.6 | 14.8 |
| **27** | 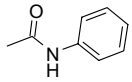 | 0.020 | >10 | 12.1 |
| **28** | 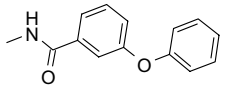 | 0.012 | >10 | 33.2 |
| **29** | 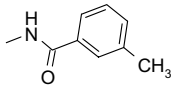 | 0.026 | >10 | 10.9 |
| **30** | 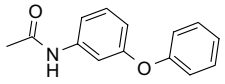 | 0.043 | >10 | 11.9 |
| **31** | 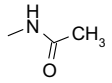 | 0.196 | >10 | >50 |
| **32** | 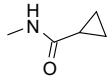 | 0.047 | >10 | 14.5 |
| **33** | 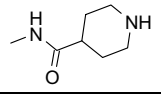 | 0.013 | >10 | 68.5 |

ND: not determined.

reduces binding affinity to 0.19 μM. Affinity could not be improved by introduction of further hydrophobic residues in **19** leading to the phenyloxy derivatives **21** and **22**. However, as demonstrated by **23** and **24**, further improvement in potency is observed when modifications are carried out with benzyloxy analogue **18**. The *meta*-chloro and methoxy derivatives **23** and **24** turned out to be approximately 6-fold more potent than its analogue **18**. This is in agreement with our models, suggesting that additional hydrophobic substituents preferably at the *meta*- or *para*-position of the distal benzyloxy ring of **18** interact with another hydrophobic subpocket on top of Ser170H-Pro170I. Additional substituents at the *meta*-position of the benzylamide ring in **18** also improved binding affinity, as exemplified for **34** (Table 3) with a $K_i$ value of 0.033 μM in comparison to **18** (0.133 μM).

Interestingly, the more polar morpholine **25** (Table 2) displayed similar activity ($K_i = 0.142$ μM) than the unsubstituted ether **18**. Again, hydrophobic substituents in *meta*-position of the central ring increase activity as illustrated by compounds **35** and **36**.

Changing the benzylether linker to a carboxamide slightly increase activity as demonstrated by compounds **26**–**33**. In addition, the high potency of **33** suggests favourable contributions by additional polar interaction at the edge of the factor VIIa binding pocket.

The complex of **29** with human factor VIIa/tissue factor was solved by X-ray structure analysis at 2.7 Å (Fig. 2), thus validating our docking hypothesis about filling the neighbourhood of the serine protease S4 subsite by hydrophobic substituents.[12] No major changes in the binding mode for the amidinophenylurea moiety of **29** were observed, compared to our previously reported X-ray structure.[4] However, the S2 pocket is now filled with a smaller, more favourable methyl substituent, which slightly affects the position of the neighbouring ligand amide bond and additionally tightens the central phenyl ring system. This central phenyl group is well ordered in

**Table 3.** In vitro activity for compounds **34**–**36**

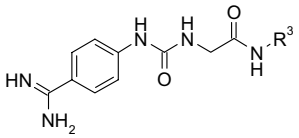

| Compounds | $R^3$ | $K_i$ (μM) | | |
|---|---|---|---|---|
| | | fVIIa | fXa | Thrombin |
| **34** | 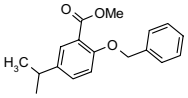 | 0.033 | >10 | 0.5 |
| **35** | 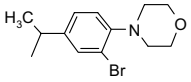 | 0.015 | >10 | 0.65 |
| **36** | 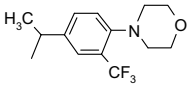 | 0.030 | >10 | 1.9 |

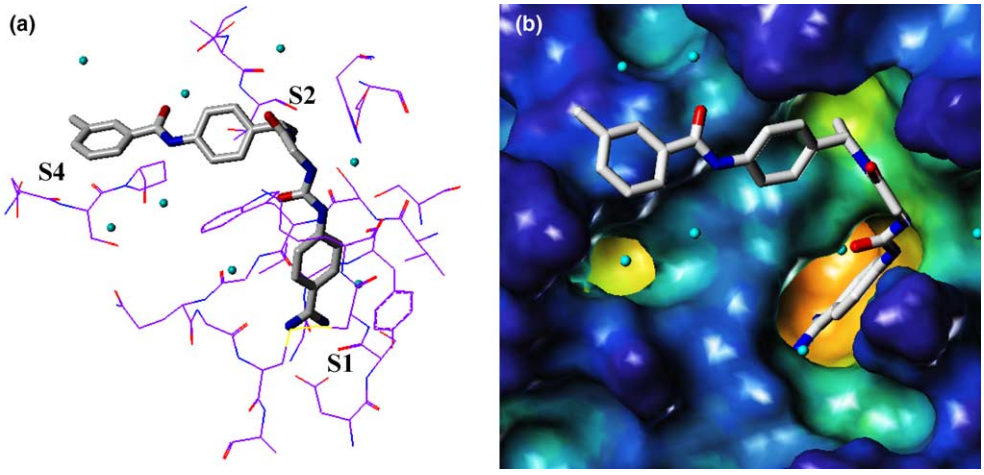


**Figure 2.** X-ray structure of compound **29** in factor VIIa/tissue factor complex at 2.7 Å resolution. Structural water molecules are indicated by cyan coloured spheres. The protein cavity on the right is represented by a MOLCAD surface coloured by subpocket depth.[11]

our electron density maps, in contrast to the crystal structure of the complex with **1**, where this phenyl group showed significant disorder. The added *meta*-methylphenyl residue does not enter the S4 pocket, but points straight ahead towards the factor VIIa loop encompassing amino acids 170B–170I. The amide carbonyl group has favourable interactions with a bound water molecule, which, in turn, is fixed by hydrogen bonds to the side chain hydroxyl and main chain nitrogen of Thr99 separating S2 and S4. This additional water mediated hydrogen bond might explain the increasing effect on affinity by replacing ether by amide linkage. The corresponding amide nitrogen is also involved in a hydrogen bond with a structurally conserved water molecule in the solvent exposed binding site region. The second methyl group again accommodates the small hydrophobic region on top of Ser170H-Pro170I, while the distal phenyl group is favourably stacked on top of Pro170I.

In summary, we have extended the structure–activity relationship of an interesting series of factor VIIa inhibitors with variations directed towards the serine protease S4 pocket and its vicinity. The best compounds (**24**, **27**, **28**, **33**, **35**) show $K_i$ values between 12 and 20 nM without significant inhibition of the related serine proteases factor Xa and thrombin. The use of structure-based design and modeling in close combination with parallel synthesis allowed us to explore rapidly structural requirements for this particular factor VIIa binding site subregion, demonstrating that the amidinophenylurea scaffold indeed constitutes a promising series for factor VIIa inhibition.

## Acknowledgements

The authors would like to thank Peter Below, Silke Herok, Iris Rein, Alexander Liesum and Andrea Struppmann for their technical assistance.

## References and notes


1. Raghavan, S. A. V.; Dikshit, M. *Drugs Future* **2002**, *27*, 669–683.
2. Ruef, J.; Katus, H. A. *Expert. Opin. Invest. Drugs* **2003**, *12*, 669–683.
3. Golino, P. *Thromb. Res.* **2002**, *106*, V257–V265.
4. Klingler, O.; Matter, H.; Schudok, M.; Bajaj, S. P.; Czech, J.; Lorenz, M.; Nestler, H. P.; Schreuder, H.; Wildgoose, P. *Bioorg. Med. Chem. Lett.* **2003**, *13*, 1463–1467.
5. South, M. S.; Case, B. L.; Wood, R. S.; Jones, D. E.; Hayes, M. J.; Girard, T. J.; Lachance, R. M.; Nicholson, N. S.; Clare, M.; Stevens, A. M.; Stegeman, R. A.; Stallings, W. C.; Kurumbail, R. G.; Parlow, J. *Bioorg. Med. Chem. Lett.* **2003**, *13*, 2319–2325.
6. Rarey, M.; Kramer, B.; Lengauer, T.; Klebe, G. *J. Mol. Biol.* **1996**, *261*, 470–489.
7. McMartin, C.; Bohacek, R. S. *J. Comput. Aided Mol. Des.* **1997**, *11*, 333–344.
8. (a) Pinner, A.; Klein, F. *Chem. Ber.* **1878**, *11*, 1825; (b) Gautier, J. A.; Miocque, M.; Farnoux, C. C. In *The Chemistry of Amidines and Imidates*; Patai, S., Ed.; Wiley: New York, 1975; pp 283–348.
9. TOTU: O-[Ethoxycarbonyl)cyanomethylenamino]-*N*,*N*,*N*′,*N*′-tetramethyl-uronium tetrafluoro-borate; König, W.; Breipohl, G.; Pokorny, P.; Birkner, M. In *Proceedings of the 21st European Peptide Symposium 1990*; Giralt, E., Andren, D., Eds.; ESCOM, Leiden, 1990; pp 143.
10. Inhibitory activity expressed as inhibition constant $K_i$ towards fVIIa/tissue factor was determined using a chromogenic assay as described in: Ostrem, J. A.; Al-Obeidi, F.; Safar, P.; Safarova, A.; Stringer, S. K.; Patek, M.; Cross, M. T.; Spoonamore, J. C.; LoCascio, J. C.; Kasireddy, P.; Thorpe, D. S.; Sepetov, N.; Lebl, M.; Wildgoose, P.; Strop, P. *Biochemistry* **1998**, *37*, 1053–1059.
11. Heiden, W.; Goetze, T.; Brickmann, J. *J. Comput. Chem.* **1992**, *14*, 246–250.
12. The factor VIIa-tissue factor complex was crystallized in hanging drops at pH 6.5 using conditions described by: Kirchhofer, D.; Guha, A.; Nemerson, Y.; Konigsberg, W. H.; Vilbois, F.; Chène, C.; Banner, D.; D'Arcy, A. *Prot. Struct. Funct. Gen.* **1995**, *22*, 419–425. Data were collected in-house on a Mar345 image plate detector mounted on a Nonius FR571 rotating anode generator, equipped with an Osmic multilayer mirror system. Data were processed with XDS: Kabsch, W. *J. Appl. Cryst.* **1993**, *26*, 795–800. The crystal diffracted to 2.7 Å with an overall $R_{sym}$ of 10.7%. The space group was $P2_12_12_1$ with $a = 69.98$ Å, $b = 81.84$ Å and $c = 126.43$ Å. Initial phases were calculated using the structure of the complex with **1**[4] as starting model, based on the original structure by Banner et al.[13] The inhibitor was fitted using Quanta and refined using CNX (Accelrys). The final *R*-factor was 17.3% (*R*-free = 24.3%). The complete inhibitor is well defined in the electron density maps.
13. Banner, D.; D'Arcy, A.; Chene, C.; Winkler, F. K.; Guha, A.; Konigsberg, W. H.; Nemerson, Y.; Kirchhofer, D. *Nature* **1996**, *380*, 41–46.